Journal of Materials Chemistry A

RSC Publishing

PAPER

View Article Online
View Journal | View Issue

Published on 13 May 2013. Downloaded by Synchrotron Radiation Library on 01/07/2013 12:10:47.

Cite this: J. Mater. Chem. A, 2013, 1, 7370

Organic photovoltaics based on a crosslinkable PCPDTBT analogue; synthesis, morphological studies, solar cell performance and enhanced lifetime†

Huw Waters,[a] Jeff Kettle,*[a] Shu-Wei Chang,[b] Chun-Jen Su,[c] Wei-Ru Wu,[c] U.-Ser Jeng,[c] Ya-Ching Tsai[b] and Masaki Horie*[b]

Received 10th March 2013
Accepted 13th May 2013

DOI: 10.1039/c3ta11002h

www.rsc.org/MaterialsA

A thermally crosslinkable poly(cyclopentadithiophene-*alt*-benzothiadiazole) (PCPDTBT) analogue copolymer with 2-ethylhexyl group and 5-hexenyl group on 4,4-positions of cyclopentadithiophene has been synthesised by palladium catalyzed Suzuki coupling reaction. Space-Charge Limited Current (SCLC) devices show hole mobility of up to 3×10^{-4} cm^2 V^{-1} s^{-1}. In addition, organic photovoltaics (OPVs) were fabricated using fullerene derivatives as acceptor materials. The best performing device exhibited Power Conversion Efficiency (PCE) at 2.0%, which could be improved to 3.7% after inclusion of dithiol additives. Most significantly, the lifetime of the OPV was enhanced by the crosslinking; when light soaked at 1 sun of irradiance, a half-life, $t_{1/2}$ = 419 hours was measured, which is 51% improvement over an OPV using standard PCPDTBT. This higher stability is accounted for the crosslinkable structure of the polymer after annealing. The crosslinking reaction was confirmed by solubility tests, Fourier transform infrared spectroscopy and morphological analysis conducted by Atomic Force Microscopy and simultaneous synchrotron grazing-incidence small-/wide-angle X-ray scattering.

1 Introduction

Solution processible organic photovoltaics (OPV) are a promising source of renewable energy and the performances of such devices have rapidly escalated since the demonstration of the first BHJ based OPV,[1,2] enabling a record efficiency of 8.3% to be recently demonstrated.[3] Despite significant research progress in the Power Conversion Efficiency (PCE) of OPVs, stability of devices remains a critical issue for commercialisation of the technology and for long-term deployment and in applications such as building-integrated photovoltaics. Techniques to improve lifetime include substituting organic hole and electron-transporting layers to metal oxides,[4,5] improved encapsulation[6,7] and synthesising polymers with a HOMO energy level below the air oxidation threshold (approximately-5.27 eV).[8] One alternative is to develop active materials that crosslink through either photo- or thermal-initiation; a number of attempts have supported this work for both donor and acceptors materials in the active layer, including the development of a photocrosslinkable derivative of the thieno[3,4-*c*]pyrrole-4,6-dione (TPD)-based polymer, which showed improved thermal stability.[9,10] A similar approach was adopted by Cheng and Hsu *et al.* and have achieved improvements in PCE as well as lifetime of OPVs, when fabricating inverted device using crosslinkable fullerene derivatives, which contained styryl groups as thermal crosslinkers.[11,12]

One of well-investigated donor polymers used in OPV fabrication is poly[4,4-bis(2-ethylhexyl)-4*H*-cyclopenta[2,1-*b*;3,4-*b*′]dithiophene-2,6-diyl-*alt*-2,1,3-benzothiadiazole-4,7-diyl](PCPDTBT) (**1**).

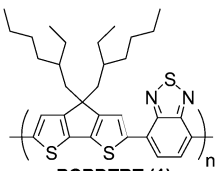

PCPDTBT (1)

The material structure consists of alternating cyclopentadithiophene donor units with benzothiadiazole acceptor units, resulting in a low optical bandgap (1.4 eV) and high performance in OFETs (μ_H = 3.3 cm^2 V^{-1} s^{-1} for the polymer with linear alkyl side groups instead of branched 2-ethylhexyl groups)[13] and OPVs (PCE = 5.5%), when blended with fullerene derivatives.[14,15] In this paper, we report the synthesis and solar cell performance of PCPDTBT with crosslinkable side chains. The purpose of this is to demonstrate a device with a high PCE, whilst improving stability. To achieve this, the 2-ethylhexyl

[a]School of Electronics, Bangor University, Dean st., Bangor, Gwynedd, LL57 1UT, Wales, UK. E-mail: j.kettle@bangor.ac.uk

[b]Frontier Research Center on Fundamental and Applied Sciences of Matters, Department of Chemical Engineering, National Tsing-Hua University, 101, Sec. 2, Kuang-Fu Road, Hsin-Chu, 30013 Taiwan. E-mail: mhorie@mx.nthu.edu.tw

[c]National Synchrotron Radiation Research Center, 101, Hsin-Ann Rd. Science Park, Hsinchu, 30076, Taiwan

† Electronic supplementary information (ESI) available. See DOI: 10.1039/c3ta11002h

This journal is © The Royal Society of Chemistry 2013

Published on 13 May 2013. Downloaded by Synchrotron Radiation Library on 01/07/2013 12:10:47.

groups were substituted with 5-hexenyl groups on the 4,4-position of cyclopentadithiophene; the crosslinking nature originates from the vinyl group of the 5-hexenyl groups. The polymer was used to fabricate Space-Charge Limited Current (SCLC) devices, in order to study the carrier mobility of the donor polymer before and after crosslinking. In addition, the polymer was used in the fabrication of OPV devices in conjunction with fullerene derivatives and the OPV performance including lifetime was studied. Devices were observed to exhibit significantly higher stability than that of the non-crosslinkable polymer, without detriment to the PCE. The crosslinking reaction of the polymers was confirmed using solubility tests and by Fourier transform infrared (FTIR) measurements. Morphological analysis was also conducted by Atomic Force Microscopy (AFM), X-ray diffraction (XRD) analysis and simultaneous synchrotron grazing-incidence small-/wide-angle X-ray scattering (GISAXS/GIWAXS).

2 Results and discussion

2.1 Synthesis

Scheme 1 shows the monomer synthesis, in which the crosslinkable side chain, 5-hexenyl group or 2-ethylhexyl branched chain were introduced onto the 4-position of cyclopentadithiophene (CPDT) through the addition of an equivalent of *n*-butyllithium followed by 6-bromo-1-hexene or 2-ethylhexylbromide. These alkylated CPDTs were then brominated by the addition of *N*-bromosuccinimide to give dibromo-CPDT with 2-ethylhexyl group (compound **2**) and dibromo-CPDT with 5-hexenyl group (compound **3**). As shown in Scheme 2, the crosslinkable random copolymers (**4** and **5**) were synthesised by palladium catalyzed Suzuki coupling reaction; polymers were synthesised with varying equivalent ratios of **2** and **3**. These ratios were varied between **2** : **3** = 95 : 5 for polymer **4** and **2** : **3** = 50 : 50 for polymer **5**. Polymers with a higher composition ratio of 5-hexenyl group were synthesised for clarification of chemical structures before and after crosslinking reaction, because the polymer with fewer vinyl groups showed insignificant change on the vinyl group in ^{1}H NMR and FT-IR measurements. Subsequent addition of excess bromobenzene or 4-bromoanisole to the reaction mixture provided phenyl- or anisole-capped polymers **6** and **7** *via* Heck coupling reaction on vinyl groups of CPDT. This allowed for a reduction in the crosslinking temperature to 160 °C.

The polymers were purified by Soxleht extraction and washed with ethanol, methylethylketone, extracted with chloroform, then filtered through silica gel column chromatography.

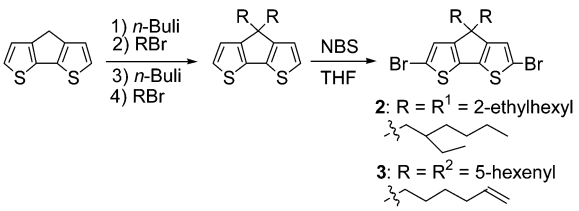

Scheme 1 Synthesis of monomers.

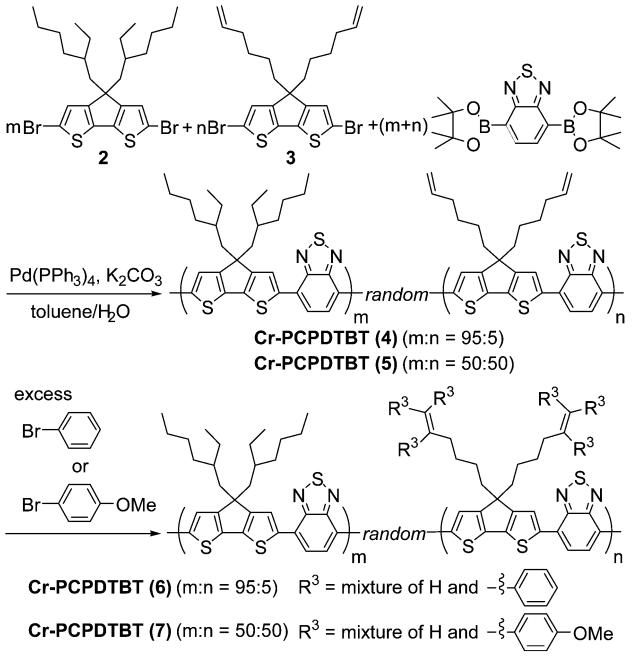

Scheme 2 Synthesis of crosslinkable PCPDTBTs.

Polymers with a higher proportion of 2-ethylhexyl side-groups (**4** and **6**) were obtained in good yield (73% and 90%, respectively) with number average molecular weight of M_n = 21 200 and polydispersity index (PDI) of 2.4 for **4** and M_n = 21 700 with PDI = 3.7 for **6**, respectively, determined by GPC measurement. In contrast, polymers with a lower proportion of 2-ethylhexyl groups (**5** and **7**) were obtained in low yield of 27% and 51%, respectively, after the Soxhlet extraction. This can be explained by the lower solubility of polymers, influenced by the reduction of solubilising side groups. Fig. 1 (top) shows ^{1}H NMR spectrum of **4** in deuterated chloroform solution. Peaks at 8.12 and 7.85 ppm are assigned to hydrogen atoms on CPDT and benzothiadiazole and small peaks at 5.71 and 4.94 ppm shown in an expansion are assigned to vinyl –CH=CH_2 of 5-hexenyl group. Other peaks around 2.1–0.6 ppm are assigned to aliphatic protons. The peak integration suggests that **4** contains 5% of the vinyl group which is consistent with initial monomer ratio. To confirm these small peaks of the vinyl group, ^{1}H NMR spectrum of **5** (50% vinyl group) was measured, in which peaks originated from vinyl –CH=CH_2 group were clearly shown at 5.82 and 4.94 ppm and the vinyl contents were estimated to be 50% from the peak integration, as shown in Fig. 1 (middle). These vinyl groups in **4** and **5** reacted with the subsequently added bromobenzene or 4-bromoanisole after the polymerisation *via* Heck reaction in the presence of palladium catalyst. Fig. 1 (bottom) shows ^{1}H NMR spectrum of **7**, in which peaks at 7.13, 6.76, 6.64 and 3.67 ppm are assigned to two aromatic protons, a vinyl proton and methoxy protons, respectively. To confirm the possibility of the Heck reaction, a model reaction was carried out between 1-octene and 4-bromoanisole under similar condition (Scheme SI-1 in the ESI†). After purifying the reaction mixture by size-exclusion liquid chromatography (SEC), the resulting product(s) was anticipated to be two anisole

Published on 13 May 2013. Downloaded by Synchrotron Radiation Library on 01/07/2013 12:10:47.

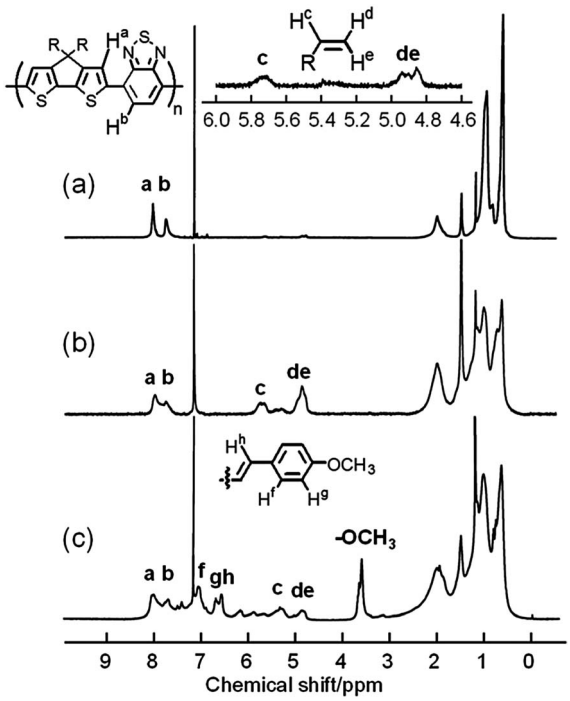

Fig. 1 ^{1}H NMR spectra (500 MHz in $CDCl_3$) of (a) **4**, (b) **5** and (c) **7**.

additives of 1-octene, which were analysed by ^{1}H NMR and mass spectra (Fig. SI-6 and SI-7†). According to ^{1}H NMR spectrum of 7 (Fig. 1 bottom), 70% of vinyl groups were capped by the anisole groups, whereas all vinyl groups were converted to phenyl groups in **6** (Fig. SI-5†).

As a comparison, a non-crosslinkable PCPDTBT (**1**) having only 2-ethylhexyl side chain was also synthesised. Details of the polymer synthesis and performance are reported elsewhere.[15] This allowed us to directly compare the effect of crosslinking in PCPDTBT device performance.

2.2 FTIR and optical absorption spectra

To test the crosslinking properties, FTIR measurements were undertaken to evaluate the properties of the synthesised polymers after crosslinking. Polymer films were prepared in glass vial and solvent was removed by rotary evaporation. Two samples were prepared and annealed at temperatures above and below the crosslinking temperatures. Fig. 2 shows FTIR spectra of **5**, which indicates absorption peaks at 993 and 910 cm^{-1} corresponding to out of plane bendings of vinyl group (–C=C–H). After annealing at 260 °C, both peaks were reduced by 32%, which demonstrates the crosslinking reaction between adjacent vinyl side groups on the polymer chains.[16] FTIR measurements were conducted for the remaining polymers and are shown in ESI-8.† Small changes in FTIR spectra before and after annealing were observed in **4** and **6** because of lower composition of crosslinking side groups, but polymer 7, which contained a large content of crosslinking units showed some evidence of crosslinking in agreement with the results for **5**.

To further demonstrate the crosslinking properties, polymers **4**–**7** were dissolved into solvent and heated until the

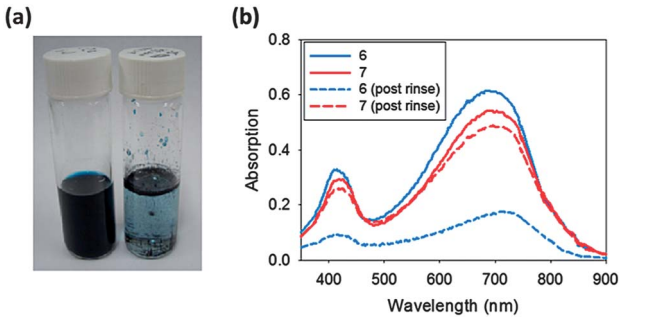

Fig. 2 (a) Photographic images of films of **7** before (left) and after (right) annealing at 160 °C and (b) absorption spectra of **6** and **7** before and after rinsing with chloroform.

polymer became insoluble. Polymer **4**, **5** and 7 became insoluble after annealing at 260 °C for 1 hour, suggesting the occurrence of a crosslinking reaction. However, polymer **6** became insoluble at 160 °C, which is a temperature more suited to OPV fabrication. In Fig. 3a the solubility of the polymer 7 before and after crosslinking polymer is shown and it can be seen the polymer is highly soluble in chlorobenzene before spin coating (left hand vial) and insoluble after annealing (right hand vial). The insolubility of polymers **4**–**6** after crosslinking is shown in ESI-9.† Due to the lower crosslinking temperature, the authors have focused on polymer **6** only. The reason for this reduction in crosslinking temperature is that polymer **6** has styryl structure given by Heck reaction (see Scheme 2). Generally, styryl groups are more reactive than allyl group and therefore, the annealing temperature is lowered.[11,12] The anisole group on polymer 7 is rather more bulky than on **6**, which might be the reason for the higher crosslinking temperature for polymer 7.

To further demonstrate the crosslinking nature of the polymers, thin films of **1**, **6** and 7 were prepared by spin coating onto glass substrates and crosslinked at their respective temperatures (160 °C for **6** and 260 °C for 7). These polymers were selected as **1** is a control, **6** in a polymer suited to OPV fabrication and 7 has a close chemical structure to **6**, but a higher crosslinking active site concentration. 1 mL of chloroform was placed on the polymer side of the glass slide for 30 seconds and dried by a high speed spinning (1000 rpm) on the coater. PCPDTBT has approximately the same solubility in chloroform

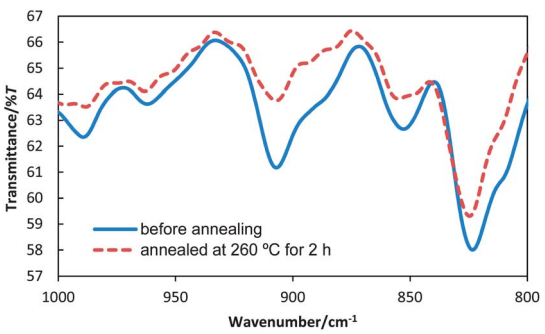

Fig. 3 FT-IR spectra (KBr) of **5** before and after annealing at 260 °C.

This journal is © The Royal Society of Chemistry 2013

Published on 13 May 2013. Downloaded by Synchrotron Radiation Library on 01/07/2013 12:10:47.

as chlorobenzene, which is later used for OPV fabrication. Thin film absorption measurements were taken before and after rinsing with chloroform and the results are shown in Fig. 3(b). Absorption spectrum for non-crosslinkable PCPDTBT (**1**) is not shown because it dissolves almost immediately in chloroform and leaves almost zero traces of the original polymer film. It is clear that the optical properties of the thin films of **6** and **7** do alter, but a large quantity of polymer remains on the glass surface. Polymer **6** maintains some solubility after crosslinking due to the lower content of 5-hexenyl groups, hence the large changed in absorption properties. Conversely, polymer **7** is only slightly affected by the solvent rinsing tests due to the higher content of 5-hexenyl groups, providing further evidence of it crosslinking nature.

2.3 Electrical and optical analysis

2.3.1 Charge transport properties. Due to the high crosslinking temperatures of **4**, **5** and **7**, device characterisation focused on polymer **6** only. The higher crosslinking temperatures poses difficulties in device analysis due to the higher crosslinking temperature; the hole transport layer used in these devices (PEDOT:PSS) is known to have a degradation temperature ~240 °C. Additionally, when preparing OPVs at 260 °C, large aggregates of PCBM are formed, which causes a reduction in the photocurrent (see ESI-10†).

Electro-optical characterisation of the synthesised materials was undertaken with a combination of Space-Charge Limited Current (SCLC) and OPV devices. SCLC current–voltage characteristics with the structure of ITO/poly(3,4-ethylenedioxythiophene): poly-(styrene sulfonate)(PEDOT:PSS)/PCPDTBT (100 nm)/Au, were made and a fit to the data was obtained using the Mott–Gurney law, enabling the hole mobility to be extracted.

Data for the dependence of hole mobility on annealing temperature is shown in Fig. 4, with the results summarised in Table 1. As described in ref. 15 and 17, SCLC devices are preferred over OFETs for evaluating mobility of semiconductors for solar cells as these materials require electronic transport in the direction perpendicular to the substrate, rather than parallel. The non-crosslinkable PCPDTBT (**1**) demonstrated a maximum mobility, $\mu_h = 2 \times 10^{-4}$ cm^2 V^{-1} s^{-1}, but decreased to 6×10^{-5} cm^2 V^{-1} s^{-1} after annealing at temperatures greater than 120 °C. This is consistent with previous experiments, which have shown the hole mobility declines with higher temperature annealing.[15]

Table 1 Hole mobility measured by Space-Charge Limited Current (SCLC) devices for a 100 nm thick film

Annealing temperature [°C]	Hole mobility [cm^2 V^{-1} s^{-1}]	
	Polymer **1**	Polymer **6**
60	2.0×10^{-4}	4.0×10^{-5}
120	8.0×10^{-5}	4.0×10^{-5}
150	6.0×10^{-5}	1.5×10^{-4}
170	5.0×10^{-5}	2.0×10^{-4}

The hole mobility of crosslinkable polymer **6** is measured at 4×10^{-5} cm^2 V^{-1} s^{-1} after annealing at low temperatures, however, this is significantly improved to be 2×10^{-4} cm^2 V^{-1} s^{-1} after annealing at temperatures greater than the crosslinking temperature of 160 °C. For this polymer, it is clear that the allyl group reduces the mobility prior to crosslinking presumably reducing the intermolecular packing between adjacent polymer chains and making efficient charge carrier transfer less favourable. However, crosslinking reduces this packing dimension, improving this charge transfer properties and, thus, the hole mobility. This view is supported by X-ray diffraction (XRD) data and GISAXS data.

2.3.2 OPV characteristics. OPVs were fabricated on glass substrates with patterned a indium tin oxide (ITO)/PEDOT:PSS anode, using 0.2 cm^2 device areas. The active layers were all spin casted from chlorobenzene solutions of the polymer **6** and PCBM with and without 1,8-octanedithiol (ODT) additives; the full procedure is outlined in Section 4.

In Fig. 5, the best performing current density–voltage curves (under AM1.5G illumination) of **6** with and without ODT are shown and the data for all experiments is summarised within Table 2. The data in Table 2 also includes data for the non-crosslinked polymer **1**, fabricated and tested under the same conditions. For all blends, the optimum polymer:fullerene blend ratio was the same as previously reported[14,15] for both material with and without ODT, but differences in optimal film thickness and annealing temperatures were discovered.

For devices fabricated from polymer **6** without ODT, the best performing devices a similar PCE to the corresponding PCPDTBT (**1**) device, despite a lower short-circuit current densities (J_{SC}) (a 6% reduction is observed). The increase in PCE is primarily due to the increase in open circuit voltage (V_{OC}) (a 6% increase) and also a minor increase in Fill Factor (FF). The lower J_{SC} correlates well to the absorption experiments (Fig. SI-11 in the ESI†), which indicated the polymer has a much lower absorption for equal film thicknesses. In fact, the measured J_{SC} is remarkably higher given the substantially lower absorption of **6**, when compared to **1**. This lower absorption property

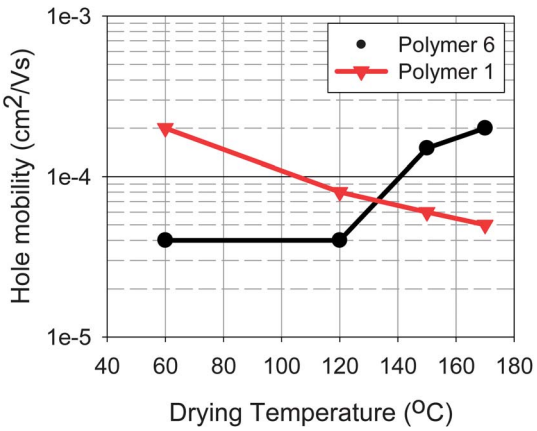

Fig. 4 Dependence of mobility of polymers **1** and **6** on annealing temperature obtained from Space-Charge Limited Current (SCLC) devices using Mott–Gurney law after annealing.

Published on 13 May 2013. Downloaded by Synchrotron Radiation Library on 01/07/2013 12:10:47.

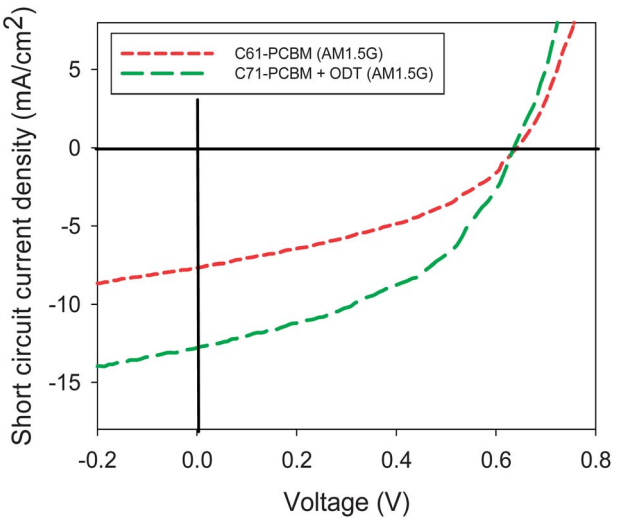

Fig. 5 Current density (*J*)–voltage (*V*) characteristics of **6**:$PC_{61}BM$ device and **6**:$PC_{71}BM$:ODT device under AM1.5G conditions and crosslinked at 170 °C. Both devices were cast from anhydrous chlorobenzene solution (30 mg mL^{-1}) and filtered prior to coating.

originates through the additional length side chains in polymer **6**. The absorption spectrum of **6** indicates that the π–π* transition is only weakly affected by the presence and positioning of the side-chains (the high energy peak does not shift), but the low-energy absorption peak does see a significantly change in relative intensity. This is assumed to be as a result of a reduced intra chain charge-transfer (CT) character from the electron-donating CPDT to the electron-accepting BT group. For devices fabricated with ODT, **6** showed a minor decrease in PCE (a 6% reduction is observed). OPV's fabricated with the crosslinked polymer also exhibited slightly lower J_{SC}. However, this drop in J_{SC} performance was partially offset by the increase in FF and V_{OC}.

For devices fabricated with and without ODT, the increase in V_{OC} with crosslinkable polymers is an interesting observation. The higher V_{OC} of the crosslinked devices (~50 mV increase), can be expected when considering the lower HOMO level of **6**; (HOMO [polymer **6**] = −4.93 eV, HOMO [polymer **1**] = −5.00 eV, from cyclic voltammograms of polymer films).

For OPV devices using polymer **1**, it was observed that annealing the active layer worsened OPV performance consistent with other ref. 15, predominantly as a result of decreases in FF and J_{SC}. The likely reason for this deterioration relates to a worse morphology for efficient charge separation and transfer and that a slow drying process improves the morphology during phase separation. This is different to the trend observed with OPVs fabricated with **6**, where consistent device performance is observed up to annealing temperatures of 160 °C. The minor improvement in FF is likely to be as a result of the increased hole mobility of **6** after annealing. The increase in hole mobility enables the series resistance, R_S to decrease, which contributes to improved charge transport properties.

Lifetime tests were carried out on OPVs fabricated with polymer **6** and **1** by blending with $PC_{71}BM$ and ODT additives. Devices were encapsulated for these tests and illuminated a 1 sun of irradiation using a light soaker. Fig. 6 shows the changes in V_{OC}, FF, J_{SC} and PCE over a 500 hours period. It is evident from the data that the solar cells fabricated with the crosslinkable polymer **6** exhibited significantly improved device performance, a half-life, $t_{1/2}$ = 450 hours was measured, which is 45% longer than that of non-crosslinked PCPDTBT. The main difference between the crosslinked and non-crosslinked OPV devices is experienced in the initial 100 hours of testing; the OPVs with crosslinked polymer appears to remain stable over this period as a small increase in performance is observed in the first 50 hours. The non-crosslinked drops off rapidly in the first 100 hours, but thereafter only experiences a slightly worse degradation rate over the remaining 400 hours of testing.

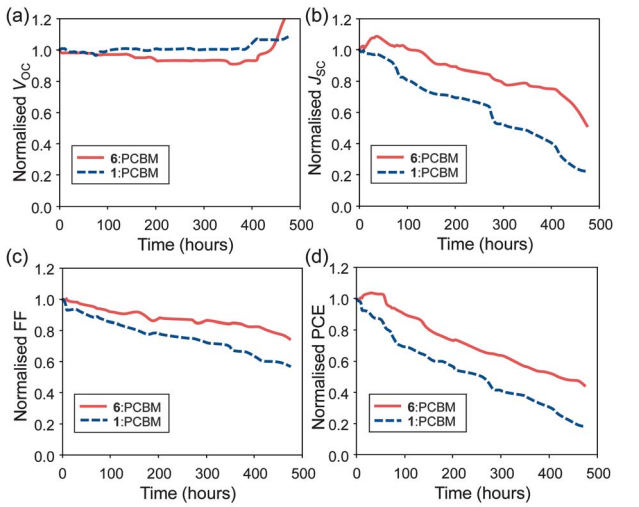

Fig. 6 Lifetime of crosslinked polymer **6**:$PC_{71}BM$:ODT device under AM1.5G conditions. Normalised photovoltaic parameters of (a) V_{OC}, (b) J_{SC}, (c) fill factor and (d) power conversion efficiency (PCE).

Table 2 OPV characteristics of polymers fabricated with $PC_{61}BM$ (ratio of polymer to fullerene = 1 : 3) or $PC_{71}BM$ (ratio of polymer to fullerene = 1 : 3.5)

Polymer	Blending (film thickness)	Annealing temperature [°C]	PCE[a] [%]	V_{oc}[b] [V]	J_{sc}[c] [mA cm^{-2}]	FF[d] [%]
6	$PC_{61}BM$ (122 nm)	160	1.84	0.650	−6.71	43.0
6	$PC_{71}BM$ + ODT (105 nm)	160	3.65	0.635	−12.8	44.8
1	$PC_{61}BM$ (125 nm)	80	1.85	0.611	−7.10	42.6
1	$PC_{71}BM$ + ODT (118 nm)	80	3.88	0.613	−13.8	44.2

[a] Power conversion efficiency measured under AM1.5G conditions. [b] Open circuit voltage. [c] Short circuit current density. [d] Fill factor.

 This journal is © The Royal Society of Chemistry 2013

Published on 13 May 2013. Downloaded by Synchrotron Radiation Library on 01/07/2013 12:10:47.

2.4 Morphological characterisation

Both the SCLC device data and OPV lifetime data clearly indicate improved thermal stability of the crosslinkable polymer, **6**. In order to understand the changes in hole mobility during crosslinking, AFM topographic scans of the polymer morphology at different annealing temperatures was undertaken and are shown in Fig. 7a–d; the micrographs showed that annealing of polymer **6** film did not show a drastic effect upon the surface roughness from (R_A = 0.563 nm, R_Z = 5.99 nm at 60 °C) to (R_A = 0.606 nm, R_Z = 6.89 nm at 170 °C). This compared to polymer **1** (micrographs not shown), where a large increase in surface roughness is observed from (R_A = 1.17 nm, R_Z = 10.5 nm) to (R_A = 1.99 nm, R_Z = 17.31 nm). The increase in surface roughness indicates large changes to the polymer morphology of the non-crosslinkable PCPDTBT after annealing, presumably indicating less thermal stability. AFM data is also shown for devices with polymer **6** blended with PCBM with 1 : 3 ratio in Fig. 7(c) and (d). After crosslinking at 170 °C, PCBM aggregation is not observed.

To understand the nature of the molecular stacking in crosslinkable polymer with PCBM, X-ray diffraction (XRD) measurements were undertaken (see Fig. 8) for **6**. XRD data for the polymer **6** shows a slightly difference molecular structure when compared to that of PCPDTBT reported elsewhere.[18]

Prior to crosslinking, the lamella packing of **6** shows a broad feature with a peak at θ = 5.12° (8.63 Å), corresponding to the branched side chains from the polymer. Despite the side chains of this analogue polymer being longer, the spacing between polymer chains is actually less than non-crosslinked 60 PCPDTBT (**1**) (θ = 4.77°, *d*-spacing = 9.27 Å). This spacing appears to increase after crosslinking. A second broad peak is also observed at θ = 11.7° (3.80 Å), due to the π-orbital stacking between polymer chains. Again, this spacing appears to increase after crosslinking. However, for both dimensions, a much stronger peak is observed in the XRD curve after crosslinking, suggesting that the crosslinking action increases the order in the polymer film. This gives some insight into the increased hole mobility of polymer **6** after crosslinking, as discussed in Section 2.3.1.

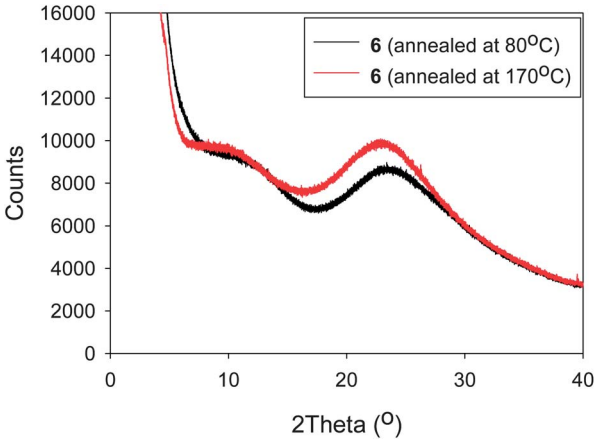

Fig. 8 XRD pattern of a 100 nm thick thin film of **6** made with (a) before and (b) after annealing at 170 °C.

For further understanding of the structural development of the crosslinkable polymers and the crosslinking effect on PCBM aggregation, we investigated *in situ* crosslinking of polymers **6** and **7** (of either 5% or 50% monomers grafted with crosslinking group), with and without PCBM, using *in situ* grazing incidence

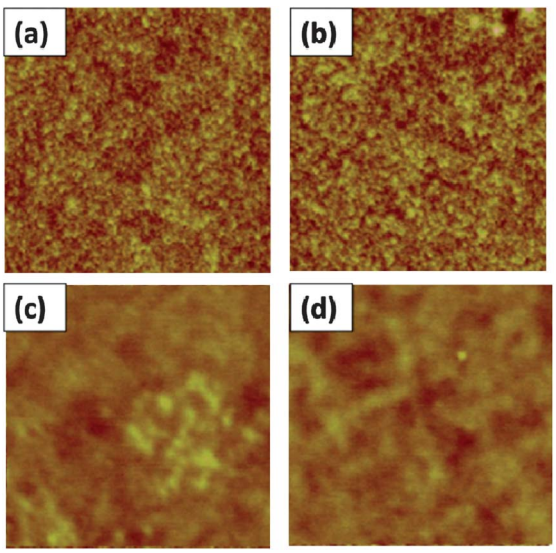

Fig. 7 AFM topography of the polymer surface of **6** (a) before and (b) after annealing at 170 °C and blended with $PC_{61}BM$ (c) before and (d) after annealing at 170 °C.

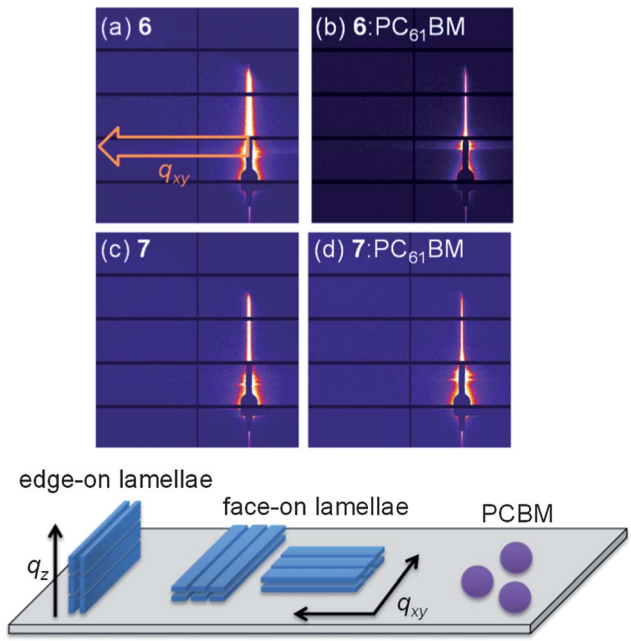

Fig. 9 GISAXS patterns of thin films of (a) **6**, (b) **6** with $PC_{61}BM$, (c) **7**, and (d) **7** with $PC_{61}BM$. Samples with **6** were annealed at 160 °C and for **7** at 260 °C for 1 hour. In-plane GISAXS profiles as a function of q_{xy} were integrated from the indicated area. Schematic image for q_{xy} and q_z with polymer lamellae and $PC_{61}BM$ is depicted.

Published on 13 May 2013. Downloaded by Synchrotron Radiation Library on 01/07/2013 12:10:47.

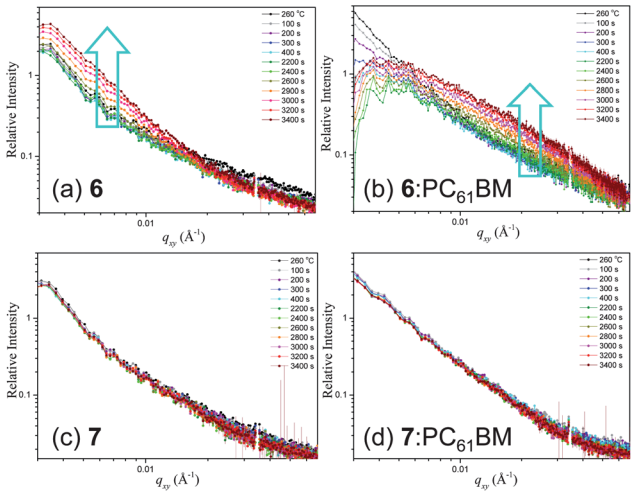

Fig. 10 In-plane GISAXS profiles of thin films of (a) **6**, (b) **6** with $PC_{61}BM$, (c) **7**, and (d) **7** with $PC_{61}BM$. All samples were annealed at 260 °C for 1 hour. The arrows in (a) and (b) depict the characteristic intensity growths in different q_{xy}-regions resulted from the conjugate polymer crosslinking and $PC_{61}BM$ aggregation, respectively.

small angle X-ray scattering (GISAXS). Shown in Fig. 9 are the 2D GISAXS patterns collected for the samples over ~1 h isothermal annealing at 160 °C (for **6**) and 260 °C (for **7**) above the crosslinking temperature. In-plane GISAXS profiles (Fig. 10) were retrieved from the specular beam position (*cf.* Fig. 9) as a function of the in-plane scattering wavevector q_{xy}. The GISAXS profile in Fig. 10a for the thin film of **6** with less crosslinking density (5%) shows successively increased intensity in the q-region of 0.004–0.02 Å^{-1} presumably owing to the formation of additionally large domains upon crosslinking. Correspondingly, GISAXS profile shown in Fig. 10b for the annealed thin film of polymer **6** revealed gradually enhanced scattering intensity in the higher q-region above 0.02 Å^{-1}, due to the characteristic $PC_{61}BM$ aggregation[19,20] of 10–20 nm size. In contrast, the GISAXS profiles observed for the film of **7** (50% crosslinkable side chains) with (Fig. 10c) or without $PC_{61}BM$ (Fig. 10d), reflect essentially no growth in the overall q-region observed. Likely, the very high crosslinking density restricted formation of additional polymer domains and suppressed completely PCBM aggregation.

3 Summary

In this paper, the synthesis of crosslinkable PCPDTBT based on cyclopentadithiophene with 5-hexenyl group and benzothiadiazole units is reported. The polymer was used to fabricate SCLC devices and the device exhibited improvements in hole mobility from 1.5×10^{-5} cm^2 V^{-1} s^{-1} to 3×10^{-4} cm^2 V^{-1} s^{-1} after crosslinking. Optimised OPVs were fabricated and tested under AM1.5G conditions after optimisation of the fabrication conditions. The best performing device shows a power conversion efficiency of 3.65%. Mostly importantly, the lifetime of the OPV device fabricated from crosslinkable PCPDTBT is significantly longer than that from PCDPTBT.

4 Experimental

4.1 General methods

All synthesis experiments were performed under an argon atmosphere using standard Schlenk techniques. Polymer molecular weight was determined by GPC in tetrahydrofuran (THF) solution using a JASCO 880-PU and a JASCO 870-UV detector (referenced to polystyrene standards). ^{1}H NMR spectra were obtained using a Bruker 500 MHz spectrometer. UV-Vis absorption spectra were recorded on a Hitachi U-3300 UV-Vis spectrophotometer. Cyclic voltammetry was performed at 0.10 V s^{-1} in a DY2300 electrochemical analyzer with a three-electrode cell, Ag/AgCl as reference electrode, platinum wire as counter electrode and polymer film on a platinum plate as the working electrode in nitrogen-purged anhydrous 0.10 M tetrabutylammonium hexafluorophosphate acetonitrile solution at room temperature. FT-IR spectra were recorded using PerkinElmer RXI FT-IR spectrometer. XRD patterns were recorded by Philips X'Pert 3040/50 diffractometer using CuKα1 (1.54060 Å) irradiation. AFM images were taken using a DI Nanoscope IIIa probe.

4.2 Synthesis of4,4-bis(5-hexenyl)-4*H*-cyclopenta[2,1-*b*;3,4-*b*′]-dithiophene

4*H*-Cyclopenta[2,1-*b*;3,4-*b*′]dithiophene (0.500 g, 2.81 mmol) was dissolved in 14 mL of anhydrous THF. *n*-Butyllithium 1.6 M in hexane (1.76 mL, 2.82 mmol) was added dropwise at −40 °C. The resulting solution was stirred at −40 °C for 1.0 hours and then at room temperature for 1.0 hours. It was then cooled to −40 °C and 6-bromo-1-hexene (0.458 g, 2.81 mmol) was added dropwise. The resulting mixture was stirred at −40 °C for 30 minutes, then it was allowed to warm to room temperature. The second alkylation was continued by following procedure. The solution was cooled to −40 °C and *n*-butyllithium 1.6 M in hexane (1.76 mL) was added dropwise at −40 °C. The resulting solution was stirred at −40 °C for 1.0 hours and then at room temperature for 1.0 hours. It was then cooled to −40 °C and 6-bromo-1-hexene (0.458 g, 2.81 mmol) was added dropwise. The resulting mixture was stirred at −40 °C for 1 hour, then it was allowed to warm to room temperature. After THF was removed under vacuum, the product was dissolved in hexane and purified by column chromatography on silica gel using hexane as the eluent. Furthermore, the product was purified by preparative size exclusion chromatography (SEC) using chloroform as the light yellow oil (0.610 g, 63%). ^{1}H NMR (500 MHz, $CDCl_3$): δ 7.13 (d, J = 5 Hz, 2H, 2-CPDT), 6.90 (d, J = 5 Hz, 2H, 3-CPDT), 5.68 (m, 2H, –C*H*=CH_2), 4.89 (d, J = 17 Hz, 2H, –CH=C*H*$_2$), 4.85 (d, J = 10 Hz, 2H, –CH=C*H*$_2$), 1.88 (qua., J = 7.5 Hz, 4H, CH_2), 1.82 (m, 4H, CH_2), 1.21 (qui., J = 7.5 Hz, 4H, CH_2), 0.94 (m, 4H, CH_2). ^{13}C NMR (125 MHz, $CDCl_3$): δ 157.9, 138.9, 136.5, 124.5, 121.6, 114.1 (CH), 53.1 (4-CPDT), 37.5, 33.5, 29.2, 24.0 (CH_2). FABMS: m/z = 343 [M + 1]$^+$.

4.3 Synthesis of 2,6-dibromo-4,4-bis(5-hexenyl)-4*H*-cyclopenta-[2,1-*b*;3,4-*b*′]dithiophene (3)

4,4-Bis(5-hexenyl)-4*H*-cyclopenta[2,1-*b*;3,4-*b*′]dithiophene (0.300 g, 0.88 mmol) was dissolved in 5.0 mL of THF. *N*-Bromosuccinimide (0.320 g, 1.76 mmol) was dissolved in 5.0 mL of THF and

 This journal is © The Royal Society of Chemistry 2013

Published on 13 May 2013. Downloaded by Synchrotron Radiation Library on 01/07/2013 12:10:47.

added dropwise at 0 °C. The resulting solution was stirred for an hour. After THF was removed under vacuum, the product was dissolved in hexane and purified by column chromatography on silica gel using hexane as the eluent. Furthermore, the product was purified by preparative SEC using chloroform as the eluent. The product was obtained as light yellow solid (0.405 g, 92% yield). ^{1}H NMR (500 MHz, $CDCl_3$): δ 6.90 (s, 2H, 3-CPDT), 5.68 (m, 1H, –C*H*=CH_2), 4.89 (m, 2H, –CH=CH_2), 1.90 (qua., 2H, CH_2); 1.75 (qui., 2H, CH_2), 1.21 (qui., 2H, CH_2), 0.91 (qui., 2H, CH_2). ^{13}C NMR (125 MHz, $CDCl_3$): δ 155.7, 138.7, 136.4, 124.5, 114.3, 111.2 (CH), 54.9 (4-CPDT), 37.3, 33.4, 29.1, 23.9 (CH_2). FABMS: m/z = 500 $[M]^+$.

4.3.1 Synthesis of polymer 4. 2,6-Dibromo-4,4-bis(2-ethylhexyl)-4*H*-cyclopenta[2,1-*b*;3,4-*b*′]dithiophene (0.150 g, 0.268 mmol), 2,6-dibromo-4,4-bis(5-hexenyl)-4*H*-cyclopenta[2,1-*b*;3,4-*b*′]dithiophene (0.006 g, 0.013 mmol), and 2,1,3-benzothiadiazole-4,7-bis(boronic acid pinacol ester) (0.113 g, 0.292 mmol), K_2CO_3 aqueous solution (1.0 mL, 1.0 M) and 2 drops of Aliquat336 were dissolved in 3.0 mL xylenes in a 25 mL Schlenk tube. The solution was purged with argon for 30 minutes, then tetrakis(triphenylphosphine) palladium(0) (0.015 g, 0.013 mmol) was added. The reaction mixture was stirred at 85 °C for 3 days. The resulting mixtures were then poured into 90 mL methanol containing 4 mL of 37 wt% hydrochloric acid. The precipitate was washed by Soxhlet extraction with ethanol and methylethylketone for a day, respectively, and then extracted with chloroform. The chloroform solution of the polymer was filtered through a flash column of silica gel and then precipitated into methanol. The precipitate was collected using centrifugation at 6000 rpm for 1 minute and the solid dried in vacuum to yield a deep blue powder (82 mg, 73% yield). ^{1}H NMR (500 MHz, $CDCl_3$): δ 8.12 (s, 2H, 3-CPDT), 7.85 (s, 2H, benzothiadiazole), 5.71 (br, 0.1H, –C*H*=CH_2), 4.94 (br, 0.1H, –CH=CH_2), 4.86 (br, 0.1H, –CH=CH_2), 2.06 (br, 4H, CH_2), 1.40–0.80 (m, CH and CH_2), 0.67 (m, 12H, CH_3). GPC: M_n = 21 200; M_w/M_n = 2.37.

4.3.2 Synthesis of polymer 5. Polymer **5** was synthesized by similar procedures to polymer **4**. 2,6-Dibromo-4,4-bis(2-ethylhexyl)-4*H*-cyclopenta[2,1-*b*;3,4-*b*′]dithiophene (0.030 g, 0.054 mmol), 2,6-dibromo-4,4-bis(5-hexenyl)-4*H*-cyclopenta[2,1-*b*;3,4-*b*′]dithiophene (0.027 g, 0.054 mmol), 2,1,3-benzothiadiazole-4,7-bis(boronic acid pinacol ester) (0.044 g, 0.112 mmol), K_2CO_3 aqueous solution (0.3 mL, 2.0 M), 1 drop of Aliquat336, tetrakis(triphenylphosphine)palladium(0) (0.006 g, 0.005 mmol), 1.5 mL xylenes. Deep blue powder (15 mg, 27%). ^{1}H NMR (500 MHz, $CDCl_3$): δ 8.08 (s, 2H, 3-CPDT), 7.85 (s, 2H, benzothiadiazole), 5.82 (br, 1H, –C*H*=CH_2), 4.94 (br, 2H, –CH=CH_2), 2.04 (br, 4H, CH_2), 1.60–0.90 (m, CH and CH_2), 0.90–0.60 (m, 6H, CH_3). GPC: M_n = 15100; M_w/M_n = 2.36.

4.3.3 Synthesis of polymer 6. Polymer **6** was synthesized by similar procedures to polymer **4**. 2,6-Dibromo-4,4-bis(2-ethylhexyl)-4*H*-cyclopenta[2,1-*b*;3,4-*b*′]dithiophene (0.150 g, 0.268 mmol), 2,6-dibromo-4,4-bis(5-hexenyl)-4*H*-cyclopenta[2,1-*b*;3,4-*b*′]dithiophene (0.007 g, 0.013 mmol), 2,1,3-benzothiadiazole-4,7-bis(boronic acid pinacol ester) (0.113 g, 0.292 mmol), K_2CO_3 aqueous solution (1.0 mL, 1.0 M), 2 drops of Aliquat336, tetrakis-(triphenylphosphine)palladium(0) (0.016 g, 0.013 mmol), 3.0 mL xylenes. In addition, after the polymerization, benzeneboronic acid 2,2-dimethyltrimethylene ester (1.0 mL) was subsequently added and stirred for 8 hours followed by the addition of 4-bromobenzene (1.0 mL). The resulting mixtures was stirred for another 8 hours and then purified by same procedure with polymer **3**. Deep blue powder (131 mg, 90%). ^{1}H NMR (500 MHz, $CDCl_3$): δ 8.12 (s, 2H, 3-CPDT), 7.85 (s, 2H, benzothiadiazole), 7.2–7.0 (m, phenyl), 6.97 (br, vinyl), 2.07 (br, 4H, CH_2), 1.40–0.90 (m, 18H, CH and CH_2), 0.67 (m, 12H, CH_3). GPC: M_n = 21 700; M_w/M_n = 3.70.

4.3.4 Synthesis of polymer 7. Polymer **7** was synthesized by similar procedures to polymer **6**. 2,6-Dibromo-4,4-bis(2-ethylhexyl)-4*H*-cyclopenta[2,1-*b*;3,4-*b*′]dithiophene (0.030 g, 0.054 mmol), 2,6-dibromo-4,4-bis(5-hexenyl)-4*H*-cyclopenta[2,1-*b*;3,4-*b*′]dithiophene (0.027 g, 0.054 mmol), 2,1,3-benzothiadiazole-4,7-bis(boronic acid pinacol ester) (0.044 g, 0.112 mmol), K_2CO_3 aqueous solution (0.3 mL, 2.0 M), 1 drop of Aliquat336, tetrakis(triphenylphosphine)palladium(0) (0.006 g, 0.005 mmol), 1.5 mL xylenes. Deep blue powder (28 mg, 51%). ^{1}H NMR (500 MHz, $CDCl_3$): δ 8.08 (s, 2H, 3-CPDT), 7.77 (s, 2H, benzothiadiazole), 7.13 (br, anisole), 6.76 (br, phenyl), 6.64 (br, vinyl), 5.40 (br, –C*H*=CH_2), 4.93 (br, –CH=CH_2), 3.67 (s, 2.4H, –OCH_3), 2.07 (br, CH_2), 1.55–1.00 (m, CH and CH_2), 0.69 (br, 6H, CH_3). GPC: M_n = 24 700; M_w/M_n = 3.09.

4.4 Fabrication of Space-Charge Limited Current (SCLC) devices

ITO coated fused silica substrates were cleaned sequentially with acetone and isopropanol using an ultrasonic bath, and dried under nitrogen atmosphere. The cleaned substrates were then spin-coated at 5000 rpm with poly(ethylene dioxythiophene) doped with polystyrene sulfonic acid, PEDOT:PSS (Ossila), from an aqueous solution and annealed at 120 °C for 20 minutes. Polymers were dissolved into anhydrous chlorobenzene at 20 mg mL^{-1} and was used to coat a 100 nm thick polymer layer. Finally, an 80 nm thick gold electrode was added by thermal evaporation. Annealing was performed prior to contact evaporation in a nitrogen glovebox. Measurements were taken using a calibrated Source Measurement Unit (SMU).

4.5 Fabrication of OPVs

ITO substrates were prepared as in Section 4.6, with a PEDOT:PSS layer, prior to coating the active layer. Prior to coating, the polymer:fullerene blends were allowed to dissolve for 48 hours on a hot plate stirrer and filtered using a 0.45 μm PTFE filter. The chlorobenzene solutions containing polymer and PCBM with various blend composition were spun-cast using different spinning rate on to these PEDOT:PSS coated substrates. The cathode electrodes consisted of 10 nm calcium followed by 80 nm aluminium. *J–V* characteristics of these PV devices were measured under white light illumination (AM1.5) using a Oriel Newport AM1.5G solar simulator output intensity of 100 mW cm^{-2}.

Illumination for light soaking measurements was provided from a halogen light soaker supplied by GB-Sol ltd, Wales, UK and devices were biased at the Maximum Power Point (MPP) in between measurements.

Published on 13 May 2013. Downloaded by Synchrotron Radiation Library on 01/07/2013 12:10:47.

4.6 GISAXS measurement

GISAXS measurements were conducted at the 23A SWAXS end station of the National Synchrotron Radiation Research Center, Taiwan. Details of the instrument were reported previously.[21] Sample thin films were respectively placed horizontally on a hot stage for 260 °C isothermal annealing. With a 15 keV (wavelength $\lambda = 0.827$ Å) beam and an incident angle 0.2°, time-resolved *GISAXS* patterns were collected using a Pilatus 1M-F area detector situated 5015 mm from the sample position. The scattering wavevector, defined as $q = 4\pi\lambda^{-1}\sin\theta$ (with 2θ the scattering angle), was calibrated using silver behenate.

Acknowledgements

The authors thank two sources for financial support. Firstly, the National Science Council of Taiwan. Secondly, Interreg IVA Wales-Ireland for their support through the "WIN-IPT". H. W. would like to thank Bangor University for his 125 Scholarship and Dr Yanhua Hong for her assistance with AFM measurements. We would also like to thank Dr Brian Murphy, from WIT in Ireland for assistance with FTIR measurements.

References

1 T. Ameri, G. Dennler, C. Lungenschmied and C. J. Brabec, *Energy Environ. Sci.*, 2009, **2**, 347–363.
2 G. Dennler, M. C. Scharber and C. J. Brabec, *Adv. Mater.*, 2009, **21**, 1323–1338.
3 L. Dou, J. You, J. Yang, C. Chen, Y. He, S. Murase, T. Moriaty, K. Emery, G. Li and Y. Yang, *Nat. Photonics*, 2012, **6**, 180–185.
4 K. X. Steirer, P. F. Ndione, N. E. Widjonarko, M. T. Lloyd, J. Meyer, E. L. Ratcliff, A. Kahn, N. R. Armstrong, C. J. Curtis, D. S. Ginley, J. J. Berry and D. C. Olson, *Adv. Energy Mater.*, 2011, **1**, 813–820.
5 J. Kettle, H. Waters, M. Horie and S.-W. Chang, *J. Phys. D: Appl. Phys.*, 2012, **45**, 12510.
6 L. Moro, N. M. Rutherford, R. J. Visser, J. A. Hauch and C. Klepek, Organic Photovoltaics VII, *Proc. SPIE*, 2006, 6334, 63340M.
7 S. Sarkar, J. H. Culp, J. T. Whyland, M. Garvan and V. Misra, *Org. Electron.*, 2010, **11**, 1896–1900.
8 D. M. de Leeuw, M. M. J. Simenon, A. R. Brown and R. E. F. Einerhand, *Synth. Met.*, 1997, **87**, 53–59.
9 G. Griffini, J. D. Douglas, C. Piliego, T. W. Holcombe, S. Turri, J. M. J. Fréchet and J. L. Mynar, *Adv. Mater.*, 2011, **23**, 1660–1664.
10 H. J. Kim, A.-R. Han, C.-H. Cho, H. Kang, H. Cho, M. Lee, J. M. J. Fréchet, J. Hak Oh and B. J. Kim, *Chem. Mater.*, 2012, **24**, 215–221.
11 C.-H. Hsieh, Y.-J. Cheng, P.-J. Li, C.-H. Chen, M. Dubosc, R.-M. Liang and C.-S. Hsu, *J. Am. Chem. Soc.*, 2010, **132**, 4887–4893.
12 Y.-J. Cheng, C.-H. Hsieh, P.-J. Li and C.-S. Hsu, *Adv. Funct. Mater.*, 2011, **21**, 1723–1732.
13 H. N. Tsao, D. M. Cho, I. Park, M. R. Hansen, A. Mavrinskiy, D. Y. Yoon and K. Müllen, *J. Am. Chem. Soc.*, 2011, **133**, 2605–2612.
14 J. K. Lee, W. L. Ma, C. J. Brabec, J. Yuen, J. S. Moon, J. Y. Kim and A. J. Heeger, *J. Am. Chem. Soc.*, 2008, **130**, 3619–3623.
15 J. Kettle, M. Horie, L. A. Majewski, B. R. Saunders, S. Tuladhar, J. Nelson and M. L. Turner, *Sol. Energy Mater. Sol. Cells*, 2011, **95**, 2186–2193.
16 T. Fukuhara, Y. Shibasaki, S. Ando and M. Ueda, *Polymer*, 2004, **45**, 843–847.
17 I. R. Gearba, C.-Y. Nam, R. Pindak and C. T. Black, *Appl. Phys. Lett.*, 2009, **95**, 173307.
18 M. Horie, J. Kettle, C.-Y. Yu, L. A. Majewski, S.-W. Chang, J. Kirkpatrick, S. M. Tuladhar, J. Nelson, B. R. Saunders and M. L. Turner, *J. Mater. Chem.*, 2012, **22**, 381–389.
19 W.-R. Wu, U. Jeng, C.-J. Su, K.-H. Wei, M.-S. Su, M.-Y. Chiu, C.-Y. Chen, W.-B. Su, C.-H. Su and A.-C. Su, *ACS Nano*, 2011, **5**, 6233–6243.
20 M.-S. Su, C.-Y. Kuo, M.-C. Yuan, U.-S. Jeng, C. Jen Su and K. Hwa Wei, *Adv. Mater.*, 2011, **23**, 3315–3319.
21 U. Jeng, C.-H. Su, C.-J. Su, K.-F. Liao, W.-T. Chuang, Y.-H. Lai, J.-W. Chang, Y.-J. Chen, Y.-S. Huang, M.-T. Lee, K.-L. Yu, J.-M. Lin, D.-G. Liu, *et al.*, *J. Appl. Crystallogr.*, 2010, **43**, 110–121.

 This journal is © The Royal Society of Chemistry 2013